Cellular and Molecular Life Sciences (2021) 78:2199–2212
https://doi.org/10.1007/s00018-020-03630-8

ORIGINAL ARTICLE

FGF primes angioblast formation by inducing ETV2 and LMO2 via FGFR1/BRAF/MEK/ERK

Peng-Chieh Chen[1,2] · Ya-Wen Hsueh[1,2] · Yi-Hsuan Lee[3] · Hung-Wen Tsai[4] · Kuen-Jer Tsai[1,2] · Po-Min Chiang[1,2]

Received: 5 March 2020 / Revised: 28 July 2020 / Accepted: 24 August 2020 / Published online: 10 September 2020

Abstract

It is critical to specify a signal that directly drives the transition that occurs between cell states. However, such inferences are often confounded by indirect intercellular communications or secondary transcriptomic changes due to primary transcription factors. Although FGF is known for its importance during mesoderm-to-endothelium differentiation, its specific role and signaling mechanisms are still unclear due to the confounding factors referenced above. Here, we attempted to minimize the secondary artifacts by manipulating FGF and its downstream mediators with a short incubation time before sampling and protein-synthesis blockage in a low-density angioblastic/endothelial differentiation system. In less than 8 h, FGF started the conversion of $KDR^{low}/PDGFRA^{low}$ nascent mesoderm into $KDR^{high}/PDGFRA^{low}$ angioblasts, and the priming by FGF was necessary to endow endothelial formation 72 h later. Further, the angioblastic conversion was mediated by the FGFR1/BRAF/MEK/ERK pathway in mesodermal cells. Finally, two transcription factors, ETV2 and LMO2, were the early direct functional responders downstream of the FGF pathway, and ETV2 alone was enough to complement the absence of FGF. FGF's selective role in mediating the first-step, angioblastic conversion from mesoderm-to-endothelium thus allows for refined control over acquiring and manipulating angioblasts. The noise-minimized differentiation/analysis platform presented here is well-suited for studies on the signaling switches of other mesodermal-lineage fates as well.

Keywords Mesoderm · Angioblasts · Endothelium · FGF · FGFR1/BRAF/MEK/ERK · ETV2 · LMO2 · Low-density and defined differentiation system

Introduction

Endothelial cells are essential for engineering artificial organs and for research on vascular diseases [1]. However, endothelial cells are extremely difficult to expand indefinitely ex vivo without introducing exogenous genes or causing them to lose their cellular identity [2, 3]. Thus, it is useful to efficiently differentiate endothelial cells from human pluripotent stem cells (hPSCs). Endothelial cells are derived from specific populations of precursor cells, angioblasts and hemangioblasts, in the mesoderm. The hemangioblasts are able to differentiate into endothelial, vascular-wall, and blood precursor cells, while angioblasts can only form endothelial and vascular-wall cells [4]. However, these endothelial precursor cells still require the forced expression of ectopic genes for long-term expansion ex vivo [5]. Together, efforts to efficiently differentiate endothelium and its precursor cells from human pluripotent stem cells (hPSCs) and to maintain them in vitro indefinitely still suffer from technical limitations. These limitations can be

Peng-Chieh Chen and Ya-Wen Hsueh contributed equally.

Electronic supplementary material The online version of this article (https://doi.org/10.1007/s00018-020-03630-8) contains supplementary material, which is available to authorized users.

✉ Po-Min Chiang
pchiang@mail.ncku.edu.tw

1 Institute of Clinical Medicine, College of Medicine, National Cheng Kung University, No. 35, Xiaodong Rd., Tainan 70457, Taiwan

2 Research Center of Clinical Medicine, National Cheng Kung University Hospital, College of Medicine, National Cheng Kung University, Tainan, Taiwan

3 Department of Pathology, National Taiwan University Hospital, Taipei, Taiwan

4 Department of Pathology, National Cheng Kung University Hospital, College of Medicine, National Cheng Kung University, Tainan, Taiwan

addressed by obtaining a mechanical understanding of how the extracellular factors drive stepwise endothelium formation through intracellular mediators.

The extracellular growth factor FGF is known to be critical for efficient derivation of endothelial cells from the mesoderm [6–8]. FGF may exert its function through maintaining endothelial identity [9], promoting endothelial proliferation [10], or inducing hemangioblasts/angioblasts [11]. In the context of endothelium-differentiation as defined herein [7], mesodermal cells barely formed endothelial cells at colonial densities with VEGF alone. This inefficiency could have been mitigated by supplementing FGF in the colonial-density culture. The resulting significantly increased the colony number, but not the colony size or purity, of endothelium with FGF supports the hypothesis that FGF triggers mesoderm into endothelial precursor cells. However, the hypothesis awaits further mechanistic clarification because high-density or colonial differentiation methods were confounded by paracrine crosstalk. Additionally, the long lag time between FGF induction and sampling and the complexity of the system made it difficult to specify the direct fate-determining transcription factors downstream of FGF.

Here, we addressed the limitations mentioned above by (i) conducting differentiation at low cell densities (less than 1000 cells/cm^2) with insufficient time for colony formation to minimize intercellular crosstalk and by (ii) collecting samples hours after FGF induction and including a protein-synthesis blocker during differentiation to identify direct responders downstream of FGF signaling. Based on the refined system, we demonstrated that the transition from mesoderm-to-endothelium comprised distinctive mesoderm-to-angioblast and angioblast-to-endothelium stages. FGF and VEGF were both necessary and sufficient for the respective transition steps in the defined differentiation medium. In addition, FGFR1/BRAF/MEK/ERK was responsible for the angioblast formation. Finally, using an epistatic analyses, two hallmark transcription factors during endothelial differentiation, ETV2 [12] and LMO2 [13], were identified as the earliest direct targets of the FGF signaling that mediated angioblast conversion.

Materials and methods

List of materials

Human iPS cell line DF19-9-7T (WiCell); human ES cell line TW1 (Bioresource Collection and Research Center, Taiwan); human ES cell line Ch22 (National Engineering Research Center of Human Stem Cells, China); Recombinant bFGF from zebra fish was produced from zbFGF offered by James Thomson (Addgene plasmid # 12,309; https://n2t.net/addgene:12309; RRID:Addgene_12309) [14]; recombinant human vitronectin was produced from pET-3c-rhVTN-NC offered by James Thomson (Addgene plasmid # 30,226; https://n2t.net/addgene:30226; RRID:Addgene_30226); recombinant human TGF-β1 and $VEGFA_{165}$ (ACROBiosystems); Y-27632 and SB431542 (SelleckChem); recombinant human Activin A, bFGF, and $VEGFA_{121}$ (ProSpecTany TechnoGene Ltd.); E. coli-derived recombinant human Bone Morphogenetic Protein 4 (BMP-4) (PEPROTECH); Accutase (Innovative Cell Technologies); (poly(vinyl alcohol) (PVA, Sigma 360,627); CHIR99021, Doxycycline, Cycloheximide, U-73122, Sotrastaurin, Gö 6983, BAPTA-AM, cyclopiazonic acid, Stattic, H89, PD 173,074, Dabrafenib, PD 325,901, SCH772984, SP600125, eFT-508 (Cayman Chemical Company); AP1903 (ApexBio); PE Mouse Anti-Human CD31 (eBioscience); PE Mouse Anti-Human CD309/KDR, PE Mouse Anti-Human PDGFRA, PE Mouse Anti-Rat CD90/Mouse CD90.1, APC mouse Anti-Human CD43, and FITC Mouse Anti-Human CD34 (BD Biosciences); anti-V5 (clone SV5-Pk1, LifeSpan BioSciences); αGAPDH (Epitope Biotech Inc.); SUPERase•In RNase inhibitor, Maxima reverse transcriptase, hygromycin B and Halt protease inhibitor cocktail (ThermoFisher); T4 DNA ligase (Enzymatics); phi29 DNA polymerase (Lucigen); TransIT-LT1 (Mirus Bio); Red Microspheres 6.0 μm (Polysciences).

Maintenance of hPSCs and differentiation

The hPSCs were maintained in E8 medium at an initial seeding density of 1250 cells/cm^2 on cell-culture dishes precoated with 2.5 μg/cm^2 of recombinant human vitronectin [14]. The medium was replenished daily with Y-27632 (10 μM) included during the first 24 h after replating. Every 6 days, for the purpose of maintenance and mesodermal differentiation, the cells were dissociated with D-PBS (without Ca^{2+} and Mg^{2+}, DPBS) containing 0.5 mM EDTA until they detached. After detachment, the cells were added to an equal volume of DPBS containing 0.1% PVA (PBSPVA) and underwent centrifugation at 300 g for 5 min and resuspension in PBS for cell counting and seeding. For mesodermal differentiation, the hPSCs (2500 cells/cm^2) were seeded in E6 medium (basal medium, E8 minus TGF-β1 and zbFGF) plus 4.5 μM CHIR99021, 5 ng/ml Activin A, 10 μM Y-27632 for 48 h before replating. The mesoderm dissociation procedure was essentially identical to that of hPSCs, except Accutase was used instead of PBS plus EDTA.

For endothelial differentiation, the mesodermal cells induced above were dissociated as with hPSCs. The dissociated mesodermal cells were seeded into E6 basal medium containing various factors at cell densities indicated in the figure legends. The timings of harvest were stated in the figure legends. Unless otherwise indicated, the following factors/concentrations were used: bFGF: zbFGF 100 ng/

ml, VEGFA: VEGFA121 10 ng/ml, bFGFH: human bFGF 10 ng/ml; and VEGFA165: human VEGFA165 10 ng/ml. Ch22 human ES cell line was used as a default unless otherwise specified in the figure legends.

For hematopoietic differentiation in Fig. 1g–j, the mesodermal cells derived as for endothelial differentiation were seeded in hemogenic mixture (HM), which was E6 basal medium containing BMP-4 (200 ng/ml), an ALK5 inhibitor (SB431542, 10 µM), PVA (0.2% w/v), zbFGF 100 ng/ml, VEGFA121 10 ng/ml. The variations of the procedure to demonstrate the importance of FGF were presented in the figure legend of Fig. 1g.

Flow cytometry of surface proteins

To characterize the formation of endothelium and angioblasts, αCD31 (1 µl/ml), αCD34 (4 µl/ml), and αKDR (2 µl/ml) were added to the cell culture 2 h before dissociation by accutase, followed by direct flow assays. For αCD90.1 or αPDGFRA staining, the hPSCs were dissociated and pelleted as for maintenance and then resuspended in 50 µl of flow buffer (DPBS with 0.5% BSA) containing αCD90.1 (0.5 µl) or αPDGFRA (2 µl). After 20-min of incubation at ambient temperature, 150 µl of flow buffer was added to the standing solution before sample loading for the flow assays. For the quantification of cell numbers shown in Fig. 1a and f, a fixed amount (10,000) of fluorescent beads were added with accutase for normalization. The hemogenic and non-hemogenic endothelia in Fig. 1h and j were dissociated with accutase, followed by the αCD90.1 staining procedure with αCD31 (0.5 µl/50 µl), αCD34 (2 µl/50 µl), and αCD43 (2 µl/50 µl).

Flow cytometry of mRNA (PLAYR)

For mRNA quantification using flow cytometry, the dissociation and pelleting processes were identical to those for the mesodermal cells. The pellets were resuspended in 100 µl of DPBS and mixed with 100 µl of 3.2% paraformaldehyde in DPBS. After incubation for 10 min at ambient temperature, the cells were pelleted in a swing-bucket rotor at 300 *g* for 5 min and resuspended in 100 µl of ice-cold methanol. After fixation and permeation at − 20 °C for at least 10 min, the cells were stained to obtain the mRNA expression based on PLAYR (Proximity Ligation Assay for RNA) [15] with the following parameters: (1) hybridization in 1 × SSC, 2.5% vol/vol polyvinylsulfonic acid, 2 µl/ml SUPERase. In, 1% Tween 20, 0.1% bovine serum albumin (BSA) and 100 µg/mL salmon sperm DNA (ssDNA), 10% ethylene carbonate and 20 nM final of PLAYR probes (Table S1) at 40 °C for 2 h; (2) stringency wash in 2X SSC, 0.1% Tween 20, 10% ethylene carbonate, and 2 µl/ml SUPERase. In at 40 °C for 20 min; (3) bridging-oligo ligation in 1X NEB buffer 4, 2 µl/ml SUPERase. In, 1 mM ATP, 0.1% Tween 20, 100 nM each of backbone and respective insert (Table S1), and 1.5 µl/100 µl of T4 DNA ligase at 37 °C for 30 min; (4) rolling-cycle amplification in 1X NEB buffer 4, 2 µl/ml SUPERase. In, 0.2 mM dNTP, 0.1% Tween 20, and 2 µl/100 µl phi29 DNA polymerase at 40 °C overnight; (5) detection-probe hybridization in 2X SSC, 1% ethylene carbonate, 0.1% Tween 20, 0.1% BSA, 100 µg/ml ssDNA, 2 µl/ml SUPERase•In and 1 nM respective detection probe (Table S1) at 37 °C for 1 h followed by a brief wash with 5X SSC, 0.1% Tween 20, and 2 µl/10 ml SUPERase. In Cells were briefly washed twice with DPBS, 0.1% Tween 20, 2 µl/10 ml SUPERase. In between each step until sample loading for flow cytometry.

Construction of gene-targeting donor vectors

The pAAVS1-NDi-CRISPRi (Gen1) backbone for the gene-targeting donor was a gift from Bruce Conklin (Addgene plasmid # 73497; https://n2t.net/addgene:73497; RRID:Addgene_73497) [16] with the following modifications: (i) the NeoR cassette was replaced by a hygromycin-resistance cassette, and (ii) the dCas9-KRAB-P2A-mCherry was replaced with the genes of interest (GOI) listed below. For Fig. 3b–d, the GOI was FGFR1 kinase-FKBP12v36 [17] from pSH1/M-FGFR1-Fv-Fvls-E (a gift by David Spencer; Addgene plasmid # 15285; https://n2t.net/addgene:15285; RRID:Addgene_15285) with a C-terminal V5 epitope. For Fig. 4a, b, the GOI's were composed of the Thy1.1 from MSCV-FOXP3-IRES-Thy1.1 (a gift from Anjana Rao; Addgene plasmid # 17443; https://n2t.net/addgene:17443; RRID:Addgene_17443) [18] and the 97-bp shRNA-expressing cassette designed by splashRNA [19] (Table S1) after the stop codon of Thy1.1. For Fig. 4c, d, a V5-KRAB-3XGGGGS epitope-suppressor-linker cassette by custom gene synthesis (MGKPIPNPLLGLDSTSLMDAKSLTAWSRTLVTFKDVFVDFTREEWKLLDTAQQIVYRNVMLENYKNLVSLGYQLTKPDVILRLEKGEEPSNSGGGGSGGGGSGGGGS) was attached at the N-termini of ETV2 (CDS of NM_014209) and LMO2 (CDS of NM_005574). For Fig. 4e–h, a V5-epitope containing peptide (MGKPIPNPLLGLDSTIGSGEGRGSLLTCGDVEENPG) was put at the N-termini of the ETV2 and LMO2coding sequences.

For the vector co-expressing Cas9 and sgRNA for the AAVS1 locus (sgAAVS1), the target sequence (Table S1) was inserted in the BbsI-digested PX459 v2.0 vector (a gift from Feng Zhang; Addgene plasmid # 62988; https://n2t.net/addgene:62988; RRID:Addgene_62988) [20].

All cloning was performed with a Gibson assembly [21].

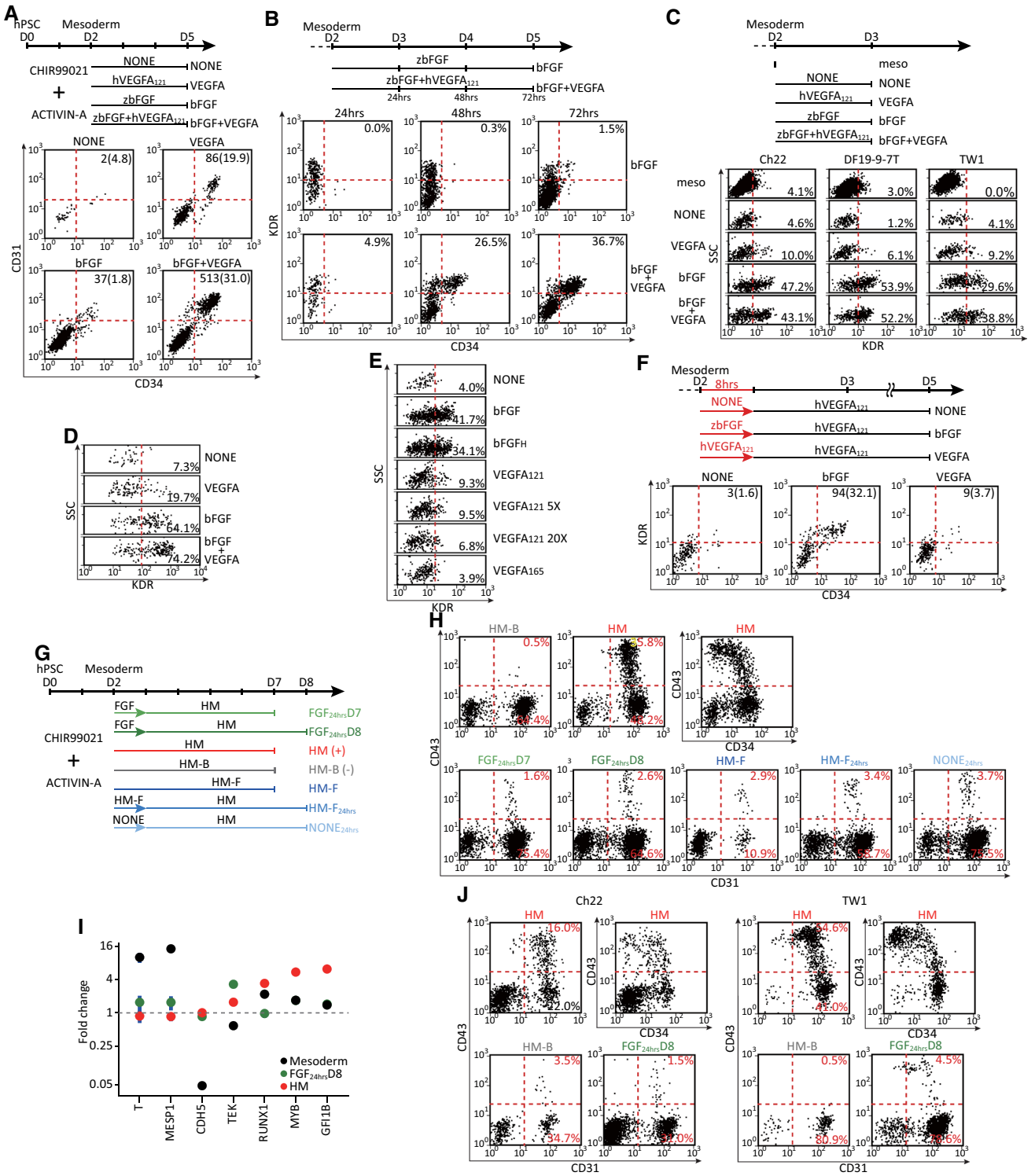

Generation of hPSC stable lines

Five µl each of the donor vector and the sgAAVS1 (0.1 µg/µl concentration) were mixed first with 87ul of the E6 medium and then with 3 µl of the TransIT-LT1 transfection reagent. The mixture was incubated at room temperature for 15 min and then transferred to a well in a 24-well plate containing 400 µl of E8 medium plus 10 µM Y-27632. After an additional 15 min, 50,000 cells of the dissociated hPSCs were seeded to the E8 medium containing the transfection complex. After 2 days, the cells were dissociated, and half of the cells were seeded into a new well in a 24-well plate

◂**Fig. 1** FGF signaling was crucial for endothelial generation through inducing KDR^{high} precursor cells. **a** Flow cytometry for mesoderm-to-endothelial induction using various growth factors. Mesodermal cells were replated (500 cells/cm^2, 2 cm^2) in basal medium with bFGF, $VEGFA_{121}$(VEGFA), both (bFGF + VEGFA) or no factors (NONE) and flowed for CD31 and CD34 expression 72 h later. **b** Flow cytometry for the emergence of KDR and CD34 immunopositive cells. Mesodermal cells were replated (250 cells/cm^2, 2 cm^2) in basal medium with bFGF or bFGF + VEGFA and flowed for KDR and CD34 expression every 24 h during days 3–5. Flow cytometry for the KDR protein (**c**, 3 independent cell lines) and mRNA (**d**) expression on day 3. Mesodermal cells were replated [500 cells/cm^2, 2 cm^2 for (**c**) and 8 cm^2 for (**d**)] in a basal medium under the conditions in **a** and assayed for KDR expression 24 h later. **e** Flow cytometry for the induction of KDR^{high} angioblasts using various sources or growth-factor concentrations. Mesodermal cells were replated (500 cells/cm^2, 2 cm^2) in basal medium with default bFGF from zebrafish (bFGF), bFGF from humans ($bFGF_H$), default human $VEGFA_{121}$ ($VEGFA_{121}$), 5- or 20-fold higher concentrations of $VEGFA_{121}$ ($VEGFA_{121}$ 5X and 20X, respectively), or a165-aa isoform of VEGFA ($VEGFA_{165}$) and assayed for KDR immunopositivity 24 h later. **f** Flow cytometry for endothelial formation after 8 h of priming with growth factors. Replated mesodermal cells (100 cells/cm^2, 2 cm^2) were incubated in basal medium with bFGF, VEGFA, or no factor (NONE) for 8 h. The medium was replaced with basal medium containing VEGFA alone for an additional 64 h and flowed for KDR and CD34 immunoreactivity. In **a** and **f**, the numbers in the right upper corners indicate the normalized numbers (percentages) of the positive cells in the double-positive populations. **g** The strategy of assaying the hemogenic potential in the mesoderm. HM (+): hemogenic mixture as the positive control; HM-B (−): HM minus BMP-4 as the negative control; HM-F: HM minus bFGF; FGF: E6 basal medium with bFGF alone; NONE: E6 basal medium alone. **h** Flow cytometry for hematopoietic differentiation under various conditions in **g**. DF19-9-7 T mesodermal cells were replated (500 cells/cm^2, 2 cm^2) and flowed for CD34, CD31 and CD43 expression after 5 days (HM, HM-B, HM-F, and FGF_{24hrs}D7) or 6 days (FGF_{24hrs}D8, $HM\text{-}F_{24hrs}$, and $NONE_{24hrs}$). **i** RT-qPCR assays for the changes of mesodermal (T, MESP1), endothelial (CDH5, TEK), and definitive hematopoietic (RUNX1, MYB, GFI1B) markers of the parental mesoderm, HM, HM-B, and FGF_{24hrs}D8 samples in **h**. The samples were harvested to obtain the relative levels of the specified mRNAs against the reference HM-B sample. The vertical bars represent 95% CI ($n = 3$). **j** Validating the loss of the hemogenic potential with the other 2 hPSC lines (Ch22 and TW1). The differentiation protocols and assay procedures were identical to those in **h**. Schematic diagrams of the experiments are on top of the data in **a**–**c**, and **f**. The induction and harvest strategies of **d** and **e** are identical to those in **c** except for the different factors/concentrations specified in **e**.

containing 400 µl of E8 medium plus 10 µM Y-27632 and 40 µg/ml of hygromycin B. The E8 medium was changed every day. The cells were selected for at least 6 days. No further colony picking was performed because we found that using this strategy, most of the surviving cells were inducible for the target proteins (Fig. 4a, e, and f).

RT-qPCR

The cells were lysed directly on culture plates by adding 50 µl of 0.2% Triton X-100 plus 200 µg/ml of proteinase K (no more than 50 seeded cells per µl of lysis buffer). The lysates were incubated at 37 °C for 30 min. Five µl of the lysates were used to prepare 10 µl Maxima RT reaction with 0.5 mM PMSF to quench the proteinase K activity, and 2.5 µM Oligo d(T)23VN was used as the RT primer. The qPCR reactions were based on SYBR (see Table S1 for the primer sequences). The fluorescence raw data were analyzed based on the R "qpcR" package [22] with the following parameters: methods = "sigfit", model = l5, type = "Cy0", which.eff = "sig", type.eff = "mean.pair", which.cp = "Cy0". The means and standard deviations from the permutation analysis were used for the statistics below.

Statistical analyses

Paired *t* test was used to demonstrate the essentiality of FGF and its intracellular mediators to induce KDR^{high} angioblasts across 3 different hPSC lines in Fig. 1c, 3e and f. For the gene-expression analysis with RT-qPCR, the permutation outputs were plotted as the fold-change means ($n = 3$) along with 95% confidence intervals for the graphic presentation. The difference was considered as statistically significant ($p < 0.05$) if the confidence intervals (CI) did not overlap with the null hypothesis of 1 (no difference). Student's *t* test was used to test the changes of PDGFRA and KDR expressions after replating the nascent mesoderm in Fig. 2e and the inhibition of various small molecules on the FGF-induced gene changes in Fig. 3g. Linear regression was used to show the dosage-dependent effect of cycloheximide on the gene expression in Fig. 2d. The statistical means ± values indicate 95% CI in the text and figures. *, and **** denote $p < 0.05$ and 0.0001, respectively.

Protein blotting

The hPSCs were dissociated and counted as for splitting. The desirable amount of cells were pelleted and resuspended in DPBS with 1% final concentration octyl glucoside and 1X Halt protease inhibitor. After incubation for 10 min on ice, the lysates were cleared by centrifugation at 17,000 *g* for 1 min, and the cleared supernatants were taken for PAGE and blotting. αV5 and αGAPDH of 1:5000 were used for staining in TBST plus 0.5% fish gelatin.

Results

FGF signaling was crucial for endothelial generation through inducing KDR^{high} precursor cells

Based on our previous method of obtaining engraftable endothelial cells in a low-density defined differentiation system, we could acquire mesodermal cells from hPSCs in E6 basal medium containing both TGFβ and canonical

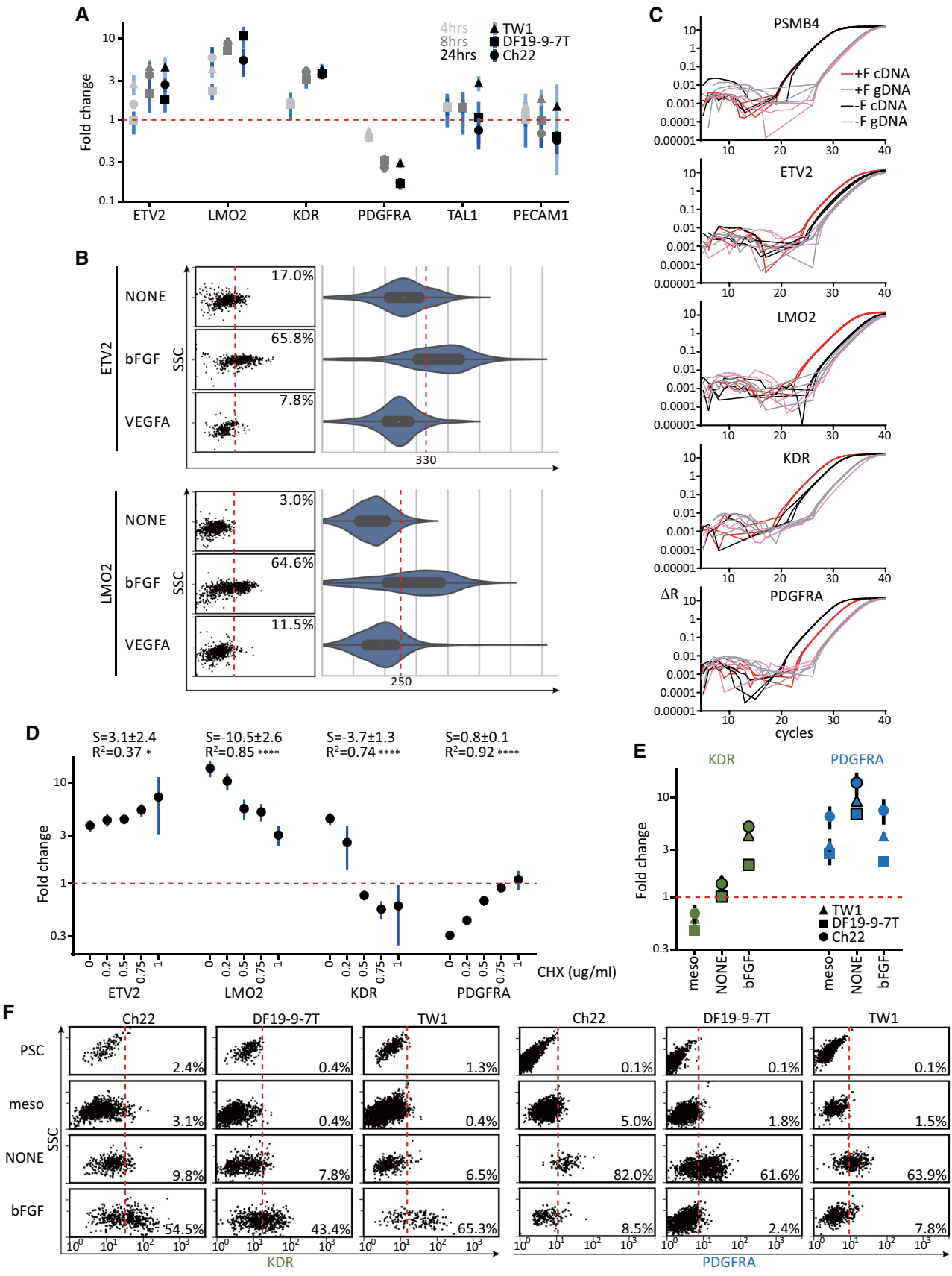
A
Fold change
4hrs
8hrs
24hrs
TW1
DF19-9-7T
Ch22
ETV2
LMO2
KDR
PDGFRA
TAL1
PECAM1
B
ETV2
NONE
bFGF
VEGFA
SSC
17.0%
65.8%
7.8%
330
LMO2
3.0%
64.6%
11.5%
250
C
PSMB4
+F cDNA
+F gDNA
-F cDNA
-F gDNA
ETV2
LMO2
KDR
ΔR
PDGFRA
cycles
D
S=3.1±2.4
R²=0.37 *
S=-10.5±2.6
R²=0.85 ****
S=-3.7±1.3
R²=0.74 ****
S=0.8±0.1
R²=0.92 ****
Fold change
CHX (ug/ml)
ETV2
LMO2
KDR
PDGFRA
E
KDR
PDGFRA
Fold change
TW1
DF19-9-7T
Ch22
meso
NONE
bFGF
F
Ch22
DF19-9-7T
TW1
PSC
meso
NONE
bFGF
SSC
2.4%
0.4%
1.3%
0.1%
0.1%
0.1%
3.1%
0.4%
0.4%
5.0%
1.8%
1.5%
9.8%
7.8%
6.5%
82.0%
61.6%
63.9%
54.5%
43.4%
65.3%
8.5%
2.4%
7.8%
KDR
PDGFRA

◂**Fig. 2** ETV2 and LMO2 were immediate genes downstream of FGF signaling. **a** RT-qPCR assays for the induction of angioblastic markers by bFGF with 3 hPSC lines. Mesodermal cells were replated (500 cells/cm^2, 2 cm^2) in basal medium with or without bFGF for 4, 8, or 24 h. The samples were harvested to obtain the relative levels (+F versus −F) of the specified mRNAs. **b** Flow cytometry for the mRNA inductions (left: dot plots; right: corresponding violin plots) of ETV2 (upper) and LMO2 (lower) after growth-factor treatments. Mesodermal cells were replated (1000 cells/cm^2, 8 cm^2) in basal medium with bFGF, VEGFA, or no factor (NONE) and assayed 8 h later. **c** Amplification curves of cDNA (red/black) and corresponding genomic DNA (pink/gray) of the same samples in **a** to reveal the background transcripts without bFGF induction. The genomic DNA for qPCR was derived by performing no-enzyme reactions side-by-side with the RT reactions for cDNA. **d** Gene-expression profiling for the inhibition of bFGF-mediated mRNA changes by blocking protein synthesis. Mesodermal cells were replated (500 cells/cm^2, 2 cm^2) in basal medium with bFGF, the concentrations of cycloheximide (CHX) were increased, and they were harvested for the RT-qPCR of the specified mRNAs 8 h later. *S* and R^2, respectively, denote mean ± 95% CI of the slope and *R*-squared of the regression line. RT-qPCR (**e**) and flow-cytometry (**f**) assays for the KDR and PDGFRA expressions from day-0 PSC to day-3 FGF-uninduced and -induced mesodermal cells across 3 hPSC lines. The strategy of differentiation was identical to that in Fig. 1c. PSC: parental hPSC cells harvested on day 0; meso: mesodermal cells harvested on day 2 before replating; NONE: E6 basal medium alone on day 3; bFGF: E6 basal medium plus bFGF on day 3. For the qPCR analyses in **a**, **d** and **e**, PSMB4 served as the reference gene. For **a** and **d**, the no-bFGF samples served as the control samples; for **e**, the PSC samples served as the control sample. Relative levels of the specified mRNAs that are significantly different ($p < 0.05$) from the day-2 nascent mesodermal cells are highlighted with black borders in **e**. The points and vertical lines represent, respectively, mean and 95% CI ($n = 3$)

WNT agonists. These differentiated cells showed increased expressions of mesenchymal markers, such as CDH2, VIM, ITGB1, FN1, ZEB, SNAI2 and TWIST1. The mesodermal nature of these cells was further verified by the surface positivity of PDGFRA and by the relative enrichment of mesodermal markers, such as T and HAND1, compared with the parental hPSCs or progeny endothelial cells [7]. In the low-density defined differentiation system, mesodermal cells could only form CD31+/CD34+ endothelial cells efficiently in the presence of both basic FGF (bFGF) and VEGF (Fig. 1a, CD31+/CD34+ cells, bFGF + VEGFA versus the others). The quantitative improvement with bFGF might have been due to the fact that FGF signaling improved the proliferation/survival or the formation of endothelial or their precursor cells. The possibility of improved proliferation after endothelial formation was unlikely because the endothelial-colony size was not increased with bFGF based on our previous finding [7]. To test if FGF signaling alone could convert endothelial precursor cells to the endothelium, the mesodermal cells were differentiated in bFGF alone or bFGF plus VEGF and assayed for the induction of endothelial cells every 24 h. The negligible amount of KDR^{high}/CD34 + endothelial cells with bFGF alone (Fig. 1b, KDR^{high}/CD34 + cells, bFGF versus bFGF + VEGFA) argued against the hypothesis as well. However, the small number of KDR^{high} cells in the mesoderm (Fig. 1c, meso), the appearance of the KDR^{high} population with bFGF alone 24 h after replating (Fig. 1b, upper panels) and the dramatic increase in the endothelial-colony number, but not size, with bFGF [7] suggested FGF signaling might mediate the mesoderm-to-endothelium transition by triggering the formation or proliferation/survival of KDR^{high} endothelial precursor cells. This hypothesis was supported by the induction of KDR expression on mesodermal cells with bFGF, but not with VEGF alone (Fig. 1c, bFGF 43.6 ± 14.2% versus VEGFA 8.4 ± 2.3%, $p = 0.0479$; and versus NONE 3.3 ± 2.1%, $p = 0.0367$). Besides the protein expression of KDR on the cell surface, the FGF-mediated induction of KDR mRNA using a proximity ligation assay for RNA (PLAYR) [15] corroborated the supposition (Fig. 1d, bFGF versus VEGFA and NONE). Although the expression of KDR mRNA was marginally higher with VEGF plus bFGF (Fig. 1d, bFGF + VEGFA versus bFGF), The inclusion of both factors did not further boost the percentage of KDR^{high} cells based on the surface expression (Fig. 1c bFGF + VEGFA 44.7 ± 7.7% versus bFGF 43.6 ± 14.2%, $p = 0.808$). The selective requirement for bFGF, but not VEGF, was further validated by different forms of bFGF, VEGF, and various concentrations of VEGF (Fig. 1e, bFGF versus VEGF and NONE). Further, the selective requirement of VEGF for the induction of KDR^{high}/CD34 + endothelium from the endothelial precursor cells was demonstrated 48 h after induction (Fig. 1b, 48–72 h, bFGF + VEGFA versus bFGF). Overall, the findings suggested that the transition from mesoderm-to-endothelium comprised two stages: the mesoderm-to-KDR^{high} precursor stage through FGF signaling, and the angioblast-to-endothelium stage through VEGF signaling. This supposition was again supported by that endothelial cells could only form efficiently when mesodermal cells were seeded in the presence of bFGF during the first 8 h before being replaced with the VEGF-only medium (Fig. 1f, bFGF versus VEGFA or NONE).

To test if these KDR^{high} endothelial precursor cells had hemogenic potential, we treated the day-2 nascent mesoderm with FGF for 24 h followed by incubating in a modified hemogenic mixture (HM, composed of basal medium plus BMP4, bFGF, VEGF$_{121}$, a TGFβ inhibitor, and PVA) from the murine system we developed previously [23]. When these FGF-induced KDR^{high} cells were incubated in HM for 4 or 5 days (Fig. 1g, FGF24hrsD7 and D8,), the induction levels of hematopoietic cells were very low (Fig. 1h, FGF24hrsD8, CD31 + /CD43 + , 1.8 ± 0.8%, $n = 3$). The lack of hemogenic potential in the KDR^{high} endothelial precursor cells was also demonstrated by the relatively low hematopoietic mRNA levels comparable to the parental mesoderm in the FGF24hrsD8 sample (Fig. 1i, RUNX1, MYB, and GFI1B), despite its higher expression of endothelial markers

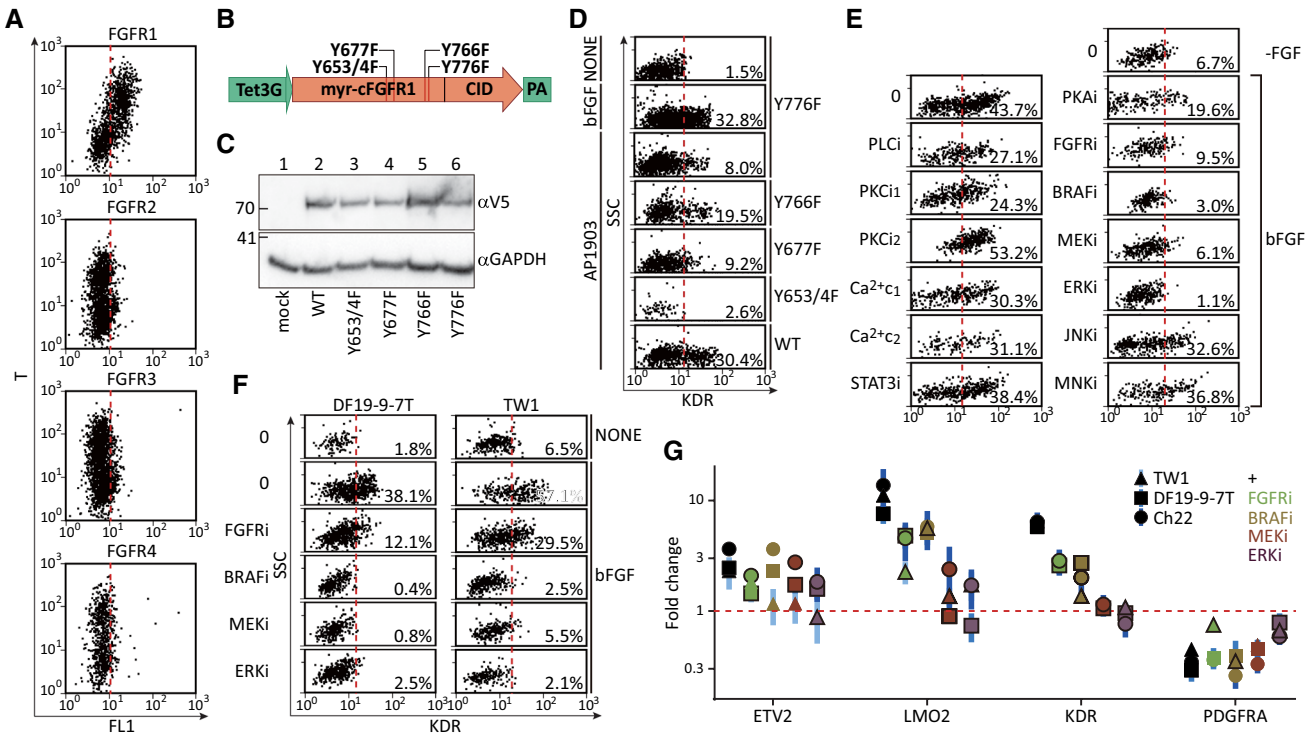

Fig. 3 FGFR1/BRAF/MEK/ERK pathway triggered the angioblastic fate. **a** Flow cytometry for the mRNA expressions of FGFR1-4 and T in day-2 mesodermal cells. hPSCs were replated (2500 cells/cm^2 precoated with 0.25 μg/ml vitronectin, 4 cm^2) in basal medium plus ACTIVIN-A (5 ng/ml) and CHIR99021 (4.5 μM) for 48 h before dissociation and fixation. The same number of 293FT cells (10,000) were mixed with the mesodermal cells at the methanol-fix step to serve as the FGFR- internal control. FGFR1-4: FAM dye; T: CY5 dye. **b** The inducible expression cassettes of the chemically-dimerizable mFGFR1 (cFGFR1) and its mutation sites for the complementation experiments in **d**. **c** Protein blotting for the induced cFGFR1s in the hygromycin-selected DF19-9-7 T hPSC lines. The inducible and parental (mock) hPSC lines (~200,000) were induced with 2 ug/ml of doxycycline for 24 h before harvesting for staining with αV5 antibody. **d** Flow cytometry for the induction of KDR expression by cFGFR1 and its mutants. The mesodermal cells were replated (500 cells/cm^2, 2 cm^2) in basal medium with AP1903 (100 nM), bFGF, or no factors (NONE) and assayed for KDR immunopositivity 24 h later. The cFGFR$_{Y776F}$ cells were used for positive (bFGF) and negative (no-factor) controls. **e** Small molecule-inhibition screening as the candidate pathways responsible for KDR induction by bFGF. Mesodermal cells were replated (500 cells/cm^2, 2 cm^2) in basal medium with bFGF alone (bFGF and 0, positive control), no factor (-FGF and 0, negative control), or bFGF plus PLCi (U-73122, 50 nM), PKCi$_1$ (Sotrastaurin 500 nM), PKCi$_2$ (Gö 6983, 1 μM), Ca^{2+} chelator 1 (Ca^{2+} c$_1$, BAPTA-AM, 1 μM), Ca^{2+} chelator 2 (Ca^{2+} c$_2$, cyclopiazonic acid, 1 μM), STAT3i (Stattic, 1 μM), PKAi (H89, 2 μM), FGFRi (PD 173074, 0.5 μM), BRAFi (Dabrafenib, 0.5 μM) MEKi (PD 325901, 20 nM), ERKi (SCH772984, 0.3 μM), JNKi (SP600125, 2 μM) or MNKi (eFT-508, 0.2 μM) and assayed as in **d**. **f** Validating the essentiality of BRAF/MAPK/ERK to induce KDR with 2 other independent hPSC lines (DF19-9-7T and TW1). The differentiation protocols, inhibitor concentrations, and assay procedures were identical to those in **e**. **g** Analysis of the suppression of angioblast-related genes by inhibiting the FGFR/BRAF/MAPK/ERK pathway. Mesodermal cells were replated and incubated as in the conditions shown in **f**. The cells were harvested 8 h after replating for RT-qPCR of the indicated genes. PSMB4 served as the reference gene, and the no-bFGF samples served as the control samples. The points and vertical lines represent, respectively, mean and 95% CI ($n=3$). Relative levels of the specified mRNAs that are significantly different ($p<0.05$) from the control FGF + samples are highlighted with black borders

(Fig. 1i, CDH5 and TEK) and the lower levels of mesodermal ones (Fig. 1i, t and MESP1, FGF24hrsD8 versus mesoderm). In contrast to the FGF-induced angioblasts, when the day-2 naïve mesodermal cells were incubated in HM (Fig. 1g, HM) for 5 days and assayed for the expressions of endothelial markers, CD31 and CD34, and a hematopoietic marker, CD43, significantly higher numbers of CD34+/CD43+ and CD31+/CD43+ cells emerged (Fig. 1h, HM, CD31+/CD43+, 34.6 ± 5.1%, $n=3$, $p=0.0002$ compared with FGF24hrsD8). Thus, the day-2 nascent mesoderm treated with HM could serve as positive control. The negative control was performed by removing an essential factor, BMP-4, from HM to abrogate the formation of the CD43+ cells (Fig. 1h, HM-B, CD31+/CD43+, 0.6 ± 0.4%, $n=3$, $p=0.0002$ compared with HM) based on our previous knowledge with the murine system. Compared with the parental mesodermal cells, both HM and HM-B samples showed increased expressions of endothelial markers, CDH5 and TEK, and decreased expressions of mesodermal ones, T and MESP1, (Fig. 1i). Besides, the HM sample showed enrichment of the definitive-hematopoiesis markers, such as RUNX1, MYB, and GFI1B, compared with the HM-B

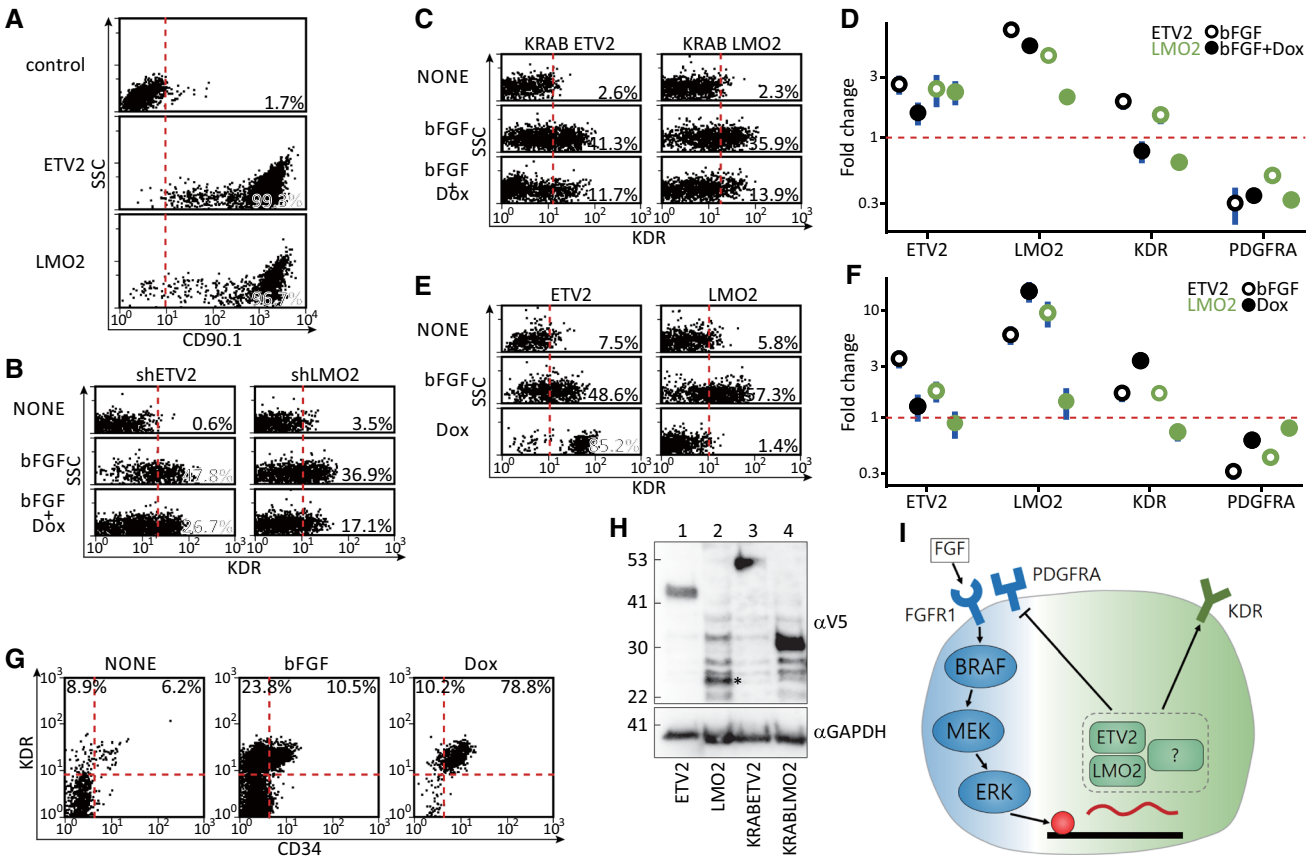

Fig. 4 ETV2 determined the angioblastic fate downstream of FGF. **a** Flow cytometry for the induction of shRNA-linked CD90.1 in hygromycin-selected DF19-9-7T lines. The parental (control) and inducible CD90.1-shETV2 and -shLMO2 hPSC lines (~200,000) were incubated with 2 ug/ml of doxycycline for 24 h before being dissociated for the surface expression of CD90.1. **b** Flow cytometry for the reduced KDR^{high} angioblasts with shRNA against ETV2 (shETV2) or LMO2 (shLMO2). Mesodermal cells were replated (1000 cells/cm^2, 2 cm^2) in basal medium with no factor (NONE), bFGF, or bFGF plus doxycycline (2 μg/ml, bFGF + Dox) and assayed for KDR immunoreactivity 24 h later. **c** Flow cytometry for the decreased KDR^{high} angioblasts by induced overexpression of suppressor KRAB-linked ETV2 (KRABETV2) or LMO2 (KRABLMO2). The procedures for the differentiation, treatment, and staining were as in **b** except that hygromycin-selected inducible KRABETV2 and KRABLMO2 cells were used. **d** Gene-expression assays for the 8-h samples in **c**. The differentiation and treatment were identical to **c** except that the samples were collected 8 h after replating the mesoderm. **e** Flow cytometry for the induction of KDR^{high} angioblasts by inducing the expression of ETV2 or LMO2. Mesodermal cells of inducible ETV2 or LMO2 were replated (1000 cells/cm^2, 2 cm^2) in basal medium with no factor (NONE), bFGF only, or doxycycline alone (2 μg/ml, Dox) and stained for KDR immunoreactivity 24 h later. **f** Gene-expression assays for the 8-h samples in **e**. The differentiation and treatment were identical to **e** and samples were collected 8 h after replating. **g** Flow cytometry for the endothelial induction after 8 h of priming of the mesoderm using bFGF or ETV2. Mesodermal cells of inducible ETV2 were replated (1000 cells/cm^2, 2 cm^2) in basal medium with no factor (NONE), bFGF, or doxycycline (2 μg/ml, Dox) for 8 h. After being washed twice with basal medium, the wells were replenished with basal medium containing $VEGFA_{121}$ (20 ng/ml) for an additional 64 h before assaying for immunoreactivity against KDR and CD34. **h** Protein blotting for the induction of ETV2, LMO2 (asterisk), KRABETV2, and KRABLMO2 in the hygromycin-selected DF19-9-7T hPSC lines. Each inducible line (~200,000) was incubated with 2 ug/ml of doxycycline for 24 h before being dissociated for immunoreactivity against the V5 epitope. For the qPCR analyses in **d**, **f**, PSMB4 served as the reference gene, and the NONE samples served as the control (baseline) samples. The points and vertical lines represent, respectively, mean and 95% CI ($n = 3$). **i** Proposed mechanism of the induction of angioblasts by FGF

sample or mesodermal cells, which further supported the presence of hemogenic endothelium in the HM positive control alone. By comparing both positive and negative controls, the lack of hemogenic potential in the KDR^{high} endothelial precursor cells was demonstrated by the relatively low hematopoietic mRNA levels (Fig. 1I, RUNX1, MYB and GFI1B, FGF24hrsD8 versus HM-B) and correspondingly few CD43+ cells comparable to the HM-B negative control (Fig. 1h and j, CD43). The lack of hemogenic potential was verified with 2 other cell lines (Fig. 1j, Ch22 and TW1). Thus, it would be proper to call the FGF-induced KDR^{high} endothelial precursor cells as angioblasts, instead of hemangioblasts, because of their endothelium-restricted fate. Nevertheless, the FGF is essential for the formation

of hemogenic endothelium based on the loss of reduction of CD31+/CD43+ cells (Fig. 1g and h, HB-F) in addition to the loss of CD31+/CD43− endothelial cells (Fig. 1g and h, HB-F) in the samples without FGF. Further, FGF was required for hematopoietic differentiation (Fig. 1g and h, CD31+/CD43+, $NONE_{24hrs}$ and $HB\text{-}F_{24hrs}$), but not for endothelial differentiation (Fig. 1g and h, CD31+/CD43−, $NONE_{24hrs}$ and $HB\text{-}F_{24hrs}$) during the first 24 h after replating mesoderm.

ETV2 and LMO2 were immediate genes downstream of FGF signaling

The increased KDR^{high} angioblasts with FGF could be explained either by FGF promoting the survival/proliferation of KDR^{high} cells or by FGF inducing fate transition from $KDR^{low/-}$ mesoderm-to-$KDR^{high/+}$ angioblasts. These hypotheses were tested by screening several genes associated with mesodermal and angioblastic fates at several time points (4, 8, and 24 h). Eight and 24 h after FGF induction, some angioblastic markers, such as ETV2, LMO2, and KDR [24], were up-regulated (Fig. 2a, 8 and 24 h). Among them, LMO2 was induced as early as 4 h post-induction (Fig. 2a, LMO2, 4 h). The induction of the transcription factors ETV2 and LMO2 in individual cells by FGF, but not VEGF, was further verified based on the mRNA flow cytometry (Fig. 2b, bFGF versus NONE and VEGFA).

A limitation of the RT-qPCR analysis was that the gene-expression levels were normalized to a house-keeping gene, PSMB4. Thus, it was impossible to see if there were basal levels of mRNA in the absence of FGF. To address this limitation, the qPCR analysis was performed with cDNA and corresponding genomic DNA samples. Again, FGF signaling obviously induced LMO2, ETV2, and KDR expression 8 h post-induction (Fig. 2c, red versus black curves). Based on the quantifications of cDNA versus genomic DNA, LMO2 was minimally expressed in the uninduced mesoderm (Fig. 2c, LMO2, black versus gray) and was strongly dependent on FGF for its expression (Fig. 2c, LMO2, red versus pink). In contrast, FGF boosted the pre-existing, basal expressions of ETV2 and KDR in the mesoderm to higher levels (Fig. 2c, ETV2, and KDR).

To identify direct responding genes downstream of FGF signaling, mesodermal cells were treated with increasing levels of cycloheximide, a translation blocker, in the presence of FGF and assayed for gene induction 8 h later. The blockage of new protein synthesis abolished the induction of KDR and the inhibition of PDGFRA by FGF signaling in a dose-dependent manner (Fig. 2d, KDR, slope = -3.7 ± 1.3, $p < 0.0001$ and CHX 1 μg/ml; PDGFRA, slope = 0.8 ± 0.1, $p < 0.0001$ and CHX 1 μg/ml). By contrast, the inductions of ETV2 (Fig. 2d, ETV2, CHX 1 μg/ml) and, to a lesser extent, LMO2 (Fig. 2d, LMO2, CHX 1 μg/ml), were minimally affected by blocking translation. Thus, the findings indicated that ETV2 and LMO2 were directly induced by FGF, and the induction of KDR and the suppression of PDGFRA were secondary to the synthesis of other mediators.

To trace the dynamics of KDR and PDGFRA expressions during the course of PSC to angioblast differentiation, we assayed the mRNA and protein expressions of the 2 genes in day-0 hPSCs, day-2 mesoderm, day-3 FGF-uninduced and -induced mesodermal cells (Fig. 2e, f, PSC, meso, NONE, and bFGF, respectively). Both KDR (more apparent in Fig. 2e, NONE versus meso) and PDGFRA (Fig. 2e, f, NONE versus meso) expressions increased when the $KDR^{low}/PDGFRA^{low}$ nascent mesoderm was incubated for 24 h in the basal medium alone without any exogenous factors. The finding suggested that either CHIR99021, ACTIVIN-A alone, or both factors in the mesoderm-differentiation medium suppressed KDR and PDGFRA expressions and the removal of the factors unleashed the suppressions in the FGF-uninduced cells. In contrast to the default no-factor condition, the incubation of FGF with the nascent mesoderm for 24 h abolished the emergence of $PDGFRA^{high}$ cells (Fig. 2e, f, bFGF versus NONE) and induced angioblasts with significant higher KDR expression compared with the no-FGF (Fig. 1c–e, 2a, c, e and f, KDR) and the nascent-mesoderm (Fig. 1c and 2e, f, KDR) samples.

Finally, the data here could not completely exclude the role of FGF in selectively promoting the survival or proliferation of KDR^{high} angioblasts at the expense of $PDGFRA^{high}$ mesodermal cells. However, the importance of FGF in diverting the default $KDR^{low}/PDGFRA^{high}$ mesodermal cells to $KDR^{high}/PDGFRA^{low}$ angioblasts was supported by the rapid induction of ETV2/LMO2 (Fig. 2a–c, ETV2, and LMO2), by the inhibition of PDGFRA expression (Fig. 2a–c, PDGFRA), and by the unchanged house-keeping PSMB4 levels when ETV2 and LMO2 were induced (Fig. 2c, PSMB4, +F versus −F).

FGFR1/BRAF/MEK/ERK pathway triggered the angioblastic fate

Because bFGF is known to trigger all four subtypes of FGFR [25], flow cytometry for the mRNA expressions of all four FGFR subtypes was performed to specify the FGF subtype that induced KDR. The expressions of FGFR2-4 were similarly low in the T + mesodermal cells and the T- cells (Fig. 3a, FGFR2-4), which were mostly 293 T cells that barely expressed any of the four FGFR subtypes [26]. In contrast, the expression of FGFR1 in the T + population was clearly higher compared to that in the T- control cells (Fig. 3a, FGFR1). To further validate the critical role of FGFR1 in specifying angioblastic fate, a dimerizing-agent inducible mouse FGFR1 (cFGFR1) [16, 17] and its tyrosine-residue mutants were used to engineer hPSC stable lines

(Fig. 3b, c, construct design and validation of protein expression, respectively). When these cell lines were differentiated into mesoderm and induced with AP1903, the dimerization inducer to activate cFGFR, the wild-type cFGFR and Y776F mutant drove KDR expression to the same degree as that by bFGF (Fig. 3d, $cFGFR_{WT}$ and $cFGFR_{Y776F}$). However, the Y653/4F, Y766F, and Y677F mutations in the activation motif of the kinase domain [27] were more or less defective in complementing the absence of bFGF (Fig. 3d. $cFGFR_{Y653/4F}$, $cFGFR_{Y766F,}$ and $cFGFR_{Y677F}$). Collectively, the findings indicated that FGFR1 induced KDR^{high} angioblasts in the mesoderm through a specific set of tyrosine residues.

To identify the intracellular pathway accounting for angioblastic induction by FGFR1, mesodermal cells were incubated with bFGF plus a panel of inhibitors against candidate mediators downstream of FGFR [28]. The blockage of PLCγ/PKC/Ca2 + (Fig. 3e, PLCi, PKCi and Ca^{2+}c), PKA (Fig. 3e, PKAi), STAT3 (Fig. 3e, STAT3i), MNK (Fig. 3e, MNKi), and JNK (Fig. 3e, JNKi) failed to suppress angioblast formation. Instead, the blockage of BRAF, MEK, and ERK (Fig. 3e, FGF 46.3 ± 11.0% versus BRAFi 2.0 ± 1.6%, $p = 0.0135$; versus MEKi 4.1 ± 3.3%, $p = 0.0123$; and versus ERKi 1.9 ± 0.8%, $p = 0.0159$) reduced the formation of KDR^{high} angioblasts to the same degree as the negative controls (Fig. 3e, FGF versus -FGF, 46.3 ± 11.0% versus 5.0 ± 3.1%, $p = 0.0125$; and versus FGFRi 17.0 ± 12.3%, $p = 0.0073$). The generality of BRAF/MEK/ERK inhibition on KDR induction was confirmed with two other hPSC cell lines (Fig. 3f). Besides its effects on the protein expression of KDR, blockage of the BRAF/MEK/ERK pathway also reduced the effects of bFGF on LMO2, KDR, ETV2 and PDGFRA. The reduction was more apparent with the components located downstream in the FGFR/BRAF/MEK/ERK pathway (Fig. 3g). Overall, the results indicated that the BRAF/MEK/ERK pathway acting downstream of FGF to convert mesoderm into angioblasts.

ETV2 and LMO2 mediated the angioblastic fate downstream of FGF

To validate the epistatic importance of ETV2 and LMO2 downstream of FGF, we designed knockdown, suppressor, and overexpression constructs of the two transcription factors and performed assays to determine their roles in angioblastic induction. The suppression of either ETV2 or LMO2 by shRNA reduced the number of KDR^{high} cells 24 h after FGF induction (see Fig. 4a and b for the percentages of shRNA-expressing cells and the induced suppression of KDR^{high} angioblasts, respectively). Because the shRNA strategy might lead to incomplete knockdown, the KRAB suppression-domain linked ETV2 and LMO2 at the N-termini (Fig. 4h, the validated protein expressions of KRABETV2 and KRABLMO2) were engineered to confirm the observation. Concurring with the shRNA results, the induction of either KRABETV2 or KRABLMO2 was detrimental to angioblastic induction by FGF (Fig. 4c, bFGF + Dox versus bFGF alone). Consistent with the protein-expression data, the mRNA levels of KDR were inhibited by either of the two suppressors 8 h after induction (Fig. 4d, KDR, bFGF + Dox versus bFGF).

To assess if either one of the transcription factors could rescue angioblast formation without FGF, the mesodermal cells were replated in basal medium alone, with bFGF, or with the doxycycline to induce either ETV2 or LMO2 (see Fig. 4h, the validated expression of ETV2 and LMO2). The overexpression of LMO2 alone failed to complement the absence of FGF in triggering KDR^{high} angioblasts (Fig. 4e, LMO2, Dox versus bFGF). The failed complementation by LMO2 was verified by the absence of changes in the mRNA 8 h after induction (Fig. 4f, LMO2, Dox). By contrast, the induction of ETV2 almost completely converted all mesodermal cells into KDR^{high} cells (Fig. 4e, ETV2, Dox versus bFGF) 24 h after induction. Additionally, ETV2 overexpression also induced the transcript levels of LMO2 and KDR, but not ETV2 itself (Fig. 4f, Dox). Besides the induction of angioblastic markers, the 8-h induction of ETV2 obliviated the FGF requirement for endothelial formation 72 h later (Fig. 4g). Remarkably, the induced ETV2 expression surpassed the effects of FGF on marker-gene induction (see Fig. 4f, LMO2 and KDR, Dox versus bFGF) as well as on angioblastic/endothelial formation (Fig. 4e and g, Dox versus bFGF).

To summarize, our observations revealed the requirement of FGF signaling for converting $PDGFRA^{low}KDR^{low}$ naïve mesoderm into $PDGFRA^{low}KDR^{high}$ angioblasts. FGFR1/BRAF/MEK/ERK were the intracellular mediators responsible for the direct induction of ETV2/LMO2. The induction of two transcription factors, especially ETV2, was critical for the fate conversion (Fig. 4i).

Discussion

With quail epiblast in vitro, KDR induction [29] and the angioblast/endothelium formation [30–32] required the presence of FGF. Contradictorily, exogenous FGF was not essential for vasculogenesis with both in vitro mouse [32] and human [7] systems. With the advantages of minimizing paracrine effects and the totally defined culture environment, our findings unify the findings across distant species and conclude the essentiality of FGF. Besides, by replacing the serum in the avian model with the defined culture medium, our study also verified the sufficiency of FGF in driving angioblasts from naïve mesoderm. Beyond FGF itself, our findings also pinpointed the specific FGFR1/BRAF/MEK/

ERK pathway and the direct downstream transcription factors for angioblast induction.

The requirement of FGF to convert mesodermal cells to angioblasts in vitro is reminiscent of in vivo gastrulation. During gastrulation, both Activin/Nodal [33] and WNT [34] signals are required for the formation of the primitive streak, which would be the in vivo counterpart of the mesodermal cells induced by Activin A and CHIR99021, a canonical Wnt agonist [35], in this study. Similar to BMP, the higher level of FGF at the posterior/proximal end [36] confers a posterolateral fate to the naïve mesoderm. The segregation of mesodermal fates by FGF is important beyond biological insights. Regarding applications, selective inclusion or blockage of FGF activity allows for the enrichment of target lineages. Thus, it would be interesting to dissect the progeny spectra of the naïve and FGF-induced mesoderms to enrich these target cell types.

The loss of hemogenic potential in bFGF-induced angioblasts 24 h after priming was caused by missing one or more of BMP-4, VEGF, SB431542, or PVA during the 24-h period. The early requirement of BMP-4 during the gastrulation stage for hematopoietic differentiation has been suggested with our murine differentiation system [23]. The early requirement for BMP-4 could be explained by the loss of an essential hemogenic licensing factor during angioblast formation, possibly due to the loss of residual Activin/WNT activity. Similar logic could also apply to the early requirement for FGF revealed in Fig. 1h or for VEGF. SB431542 could exert its effect by blocking the inhibitory activities of paracrine TGFβ or carryover ACTIVIN-A used during mesodermal induction [37]. The angioblast-enrichment potential of anti-detachment PVA [7] also possibly reduced the paracrine anti-hemogenic signal from contaminating cell types. The low-density, defined system here allows for testing these hypotheses in the future. The transcriptome comparisons between individual cells of parental mesodermal cells and their progenies induced with each and combinations of the critical factors will tell us how each signal drives particular transcription factors and how these transcription factors integrate to endow distinct cell fates and to confer hemogenic potential. The mechanistic insight will be useful for the derivation of pure cell types by direct cell-type conversion.

The selective requirement of FGF, rather than VEGF, to induce angioblasts is intriguing. KDR, the receptor required for endothelial formation [38], already existed in the naïve mesoderm (Fig. 2c). However, even the high dosages of the VEGF ligand failed to induce angioblast formation in the absence of FGF. This unresponsiveness could result from quantitative or qualitative KDR defects. Quantitatively, lower mRNA levels or inefficient translation without FGF could reduce the working KDR or KDR/FLT1 ratio on the cell surface [39]. Qualitatively, KDR might miss specific intracellular pathways, might induce downstream pathways with distinctive strength/duration [40], or might exist as an inactive form due to mislocation or other reasons. This hypotheses could be tested by manipulating the level, activity, location, or intracellular pathways of KDR in the mesoderm. Likewise, the mechanisms underlying the unique requirement of VEGF, but not FGF (Fig. 1b), in angioblast-to-endothelium conversion deserve further exploration.

When the protein synthesis was blocked, FGF's selective capability to induce ETV2 and LMO2, but not KDR (Fig. 2d), suggests the post-translational activation of a switchable transcription factor. The transcription factor is likely to be phosphorylated either directly or indirectly on the active BRAF/MEK/ERK pathway (Fig. 2e–g). If this conjecture is true, searching for the particular transcriptor factors would be stimulating. Candidates include ETS, ELK, c-Myc, etc. [41]. Because ERK is already active at the primed-pluripotency stage [42], the switchable transcription factors are likely to express selectively at the naïve mesoderm stage or require other mesoderm-specific transcription factors to mediate angioblast conversion. A mechanistic understanding would be facilitated by transcriptome profiling and comparison of the hPSCs and naïve mesodermal cells based on the culture conditions used in this study.

ETV2 and LMO2 were direct, immediate-early targets downstream of FGF signaling. Although both gene-knockdown (Fig. 4b) and the suppressor-overexpression (Fig. 4c, d) assays supported the importance of LMO2 in mediating angioblast formation, overexpression of LMO2 in the mesoderm failed to trigger changes related to angioblast-associated genes (Fig. 4e, f). The ineffectiveness of overexpressing LMO2 alone could be explained by its lack of DNA-binding activity and, thus, its requirement of other partners for its function [43]. This supposition was supported by the inhibition of angioblast formation (Fig. 3c) and KDR/LMO2 expression (Fig. 3d) when KRABLMO2 was induced in the presence of FGF. On the other hand, overexpressed ETV2 dominantly mediated almost complete angioblast conversion in naïve mesoderm (Fig. 4e–g). This dominance was demonstrated by its inclusion in transdifferentiation of the endothelial precursor cells from other cell types [5, 44, 45]. However, ETV2 was also highly expressed in non-hematoendothelial cells [46] and does not have auto-induction ability (Fig. 4f). These facts suggest the existence of cofactors for angioblast induction by ETV2. The cofactors will be revealed by assaying transcriptomes in the naïve and FGF-induced mesoderms.

Given the critical function of FGF and its downstream pathway in imparting angioblast fate in the mesoderm, manipulating the activity of this particular pathway can be used to acquire purer subpopulations of mesodermal subtypes. In addition, the direct induction of ETV2 by FGF and the complete conversion of angioblasts by overexpressing ETV2 also implies the possibility of deriving and

maintaining angioblasts using exogenous factors or small molecules. Beyond the information provided here, our low-density, short incubation-time differentiation platform will be helpful in regard to clarifying the roles of other signals in determining mesodermal lineages in general.

Author contributions PC and PC designed research; PC, YH, YL, HT, KT and PC analyzed the data; PC, YH and PC performed research; PC and PC wrote the paper; HT, KT contributed new reagents or analytic tools.

Funding The study was supported by the Ministry of Science and Technology, Taiwan (107-2314-B-006-025, 108-2320-B-006-028 and 109-2320-B-006-029).

Availability of data and material All materials are available upon request.

Compliance with ethical standards

Conflict of interest The authors declare no conflicts of interest/competing interests.

References

1. Gomez-Salinero JM, Rafii S (2018) Endothelial cell adaptation in regeneration. Science 362:1116–1117
2. Miller AZ, Satchie A, Tannenbaum AP, Nihal A, Thomson JA, Vereide DT (2018) Expandable arterial endothelial precursors from human CD34+ cells differ in their proclivity to undergo an endothelial-to-mesenchymal transition. Stem cell reports 10:73–86
3. Sandler VM, Lis R, Liu Y, Kedem A, James D, Elemento O, Butler JM, Scandura JM, Rafii S (2014) Reprogramming human endothelial cells to haematopoietic cells requires vascular induction. Nature 511:312
4. Dzierzak E, Speck NA (2008) Of lineage and legacy: the development of mammalian hematopoietic stem cells. Nat Immunol 9:129–136
5. Vereide DT, Vickerman V, Swanson SA, Chu L-F, McIntosh BE, Thomson JA (2014) An expandable, inducible hemangioblast state regulated by fibroblast growth factor. Stem Cell Rep 3:1043–1057
6. Dzierzak E, Bigas A (2018) Blood development: hematopoietic stem cell dependence and independence. Cell Stem Cell 22:639–651
7. Wu Y-T, Yu I-S, Tsai K-J, Shih C-Y, Hwang S-M, Su I-J, Chiang P-M (2015) Defining minimum essential factors to derive highly pure human endothelial cells from iPS/ES cells in an animal substance-free system. Sci Rep 5:9718
8. Olgasi C, Talmon M, Merlin S, Cucci A, Richaud-Patin Y, Ranaldo G, Colangelo D, Di Scipio F, Berta GN, Borsotti C et al (2018) Patient-specific iPSC-derived endothelial cells provide long-term phenotypic correction of hemophilia A. Stem Cell Rep 11:1391–1406
9. Dejana E, Hirschi KK, Simons M (2017) The molecular basis of endothelial cell plasticity. Nat Commun 8:14361
10. Yu P, Wilhelm K, Dubrac A, Tung JK, Alves TC, Fang JS, Xie Y, Zhu J, Chen Z, de Smet F et al (2017) FGF-dependent metabolic control of vascular development. Nature 545:224
11. Vodyanik MA, Yu J, Zhang X, Tian S, Stewart R, Thomson JA, Slukvin II (2010) A mesoderm-derived precursor for mesenchymal stem and endothelial cells. Cell Stem Cell 7:718–729
12. Liu F, Li D, Yu YYL, Kang I, Cha M-J, Kim JY, Park C, Watson DK, Wang T, Choi K (2015) Induction of hematopoietic and endothelial cell program orchestrated by ETS transcription factor ER71/ETV2. EMBO Rep 16:654–669
13. Patterson LJ, Gering M, Eckfeldt CE, Green AR, Verfaillie CM, Ekker SC, Patient R (2007) The transcription factors Scl and Lmo2 act together during development of the hemangioblast in zebrafish. Blood 109:2389–2398
14. Ludwig TE, Bergendahl V, Levenstein ME, Yu J, Probasco MD, Thomson JA (2006) Feeder-independent culture of human embryonic stem cells. Nat Methods 3:637
15. Frei AP, Bava F-A, Zunder ER, Hsieh EWY, Chen S-Y, Nolan GP, Gherardini PF (2016) Highly multiplexed simultaneous detection of RNAs and proteins in single cells. Nat Methods 13:269
16. Mandegar MA, Huebsch N, Frolov EB, Shin E, Truong A, Olvera MP, Chan AH, Miyaoka Y, Holmes K, Spencer CI et al (2016) CRISPR interference efficiently induces specific and reversible gene silencing in human iPSCs. Cell Stem Cell 18:541–553
17. Freeman KW, Gangula RD, Welm BE, Ozen M, Foster BA, Rosen JM, Ittmann M, Greenberg NM, Spencer DM (2003) Conditional activation of fibroblast growth factor receptor (FGFR) 1, but not FGFR2, in prostate cancer cells leads to increased osteopontin induction, extracellular signal-regulated kinase activation, and in vivo proliferation. Can Res 63:6237–6243
18. Wu Y, Borde M, Heissmeyer V, Feuerer M, Lapan AD, Stroud JC, Bates DL, Guo L, Han A, Ziegler SF et al (2006) FOXP3 controls regulatory T cell function through cooperation with NFAT. Cell 126:375–387
19. Pelossof R, Fairchild L, Huang C-H, Widmer C, Sreedharan VT, Sinha N, Lai D-Y, Guan Y, Premsrirut PK, Tschaharganeh DF et al (2017) Prediction of potent shRNAs with a sequential classification algorithm. Nat Biotechnol 35:350
20. Ran FA, Hsu PD, Wright J, Agarwala V, Scott DA, Zhang F (2013) Genome engineering using the CRISPR-Cas9 system. Nat Protoc 8:2281
21. Gibson DG, Young L, Chuang R-Y, Venter JC, Hutchison CA III, Smith HO (2009) Enzymatic assembly of DNA molecules up to several hundred kilobases. Nat Methods 6:343
22. Ritz C, Spiess A-N (2008) qpcR: an R package for sigmoidal model selection in quantitative real-time polymerase chain reaction analysis. Bioinformatics 24:1549–1551
23. Chiang P-M, Wong PC (2011) Differentiation of an embryonic stem cell to hemogenic endothelium by defined factors: essential role of bone morphogenetic protein 4. Development 138:2833–2843
24. Elcheva I, Brok-Volchanskaya V, Kumar A, Liu P, Lee J-H, Tong L, Vodyanik M, Swanson S, Stewart R, Kyba M et al (2014) Direct induction of haematoendothelial programs in human pluripotent stem cells by transcriptional regulators. Nat Commun 5:4372
25. Tiong KH, Mah LY, Leong C-O (2013) Functional roles of fibroblast growth factor receptors (FGFRs) signaling in human cancers. Apoptosis 18:1447–1468
26. Uhlén M, Fagerberg L, Hallström BM, Lindskog C, Oksvold P, Mardinoglu A, Sivertsson Å, Kampf C, Sjöstedt E, Asplund A et al (2015) Tissue-based map of the human proteome. Science 347:1260419
27. Ornitz DM, Itoh N (2015) The fibroblast growth factor signaling pathway. Wiley Interdiscip Rev Dev Biol 4:215–266
28. Touat M, Ileana E, Postel-Vinay S, André F, Soria J-C (2015) Targeting FGFR signaling in cancer. Clin Cancer Res 21:2684–2694
29. Flamme I, Breier G, Risau W (1995) Vascular endothelial growth factor (VEGF) and VEGF receptor 2 (flk-1) are expressed during

vasculogenesis and vascular differentiation in the quail embryo. Dev Biol 169:699–712
30. Cox CM, Poole TJ (2000) Angioblast differentiation is influenced by the local environment: FGF-2 induces angioblasts and patterns vessel formation in the quail embryo. Dev Dyn 218:371–382
31. Flamme I, Risau W (1992) Induction of vasculogenesis and hematopoiesis in vitro. Development 116:435–439
32. Risau W, Flamme I (1995) Vasculogenesis. Annu Rev Cell Dev Biol 11:73–91
33. Zhou X, Sasaki H, Lowe L, Hogan BLM, Kuehn MR (1993) Nodal is a novel TGF-\beta-like gene expressed in the mouse node during gastrulation. Nature 361:543
34. Liu P, Wakamiya M, Shea MJ, Albrecht U, Behringer RR, Bradley A (1999) Requirement for Wnt3 in vertebrate axis formation. Nat Genet 22:361
35. Ying Q-L, Wray J, Nichols J, Batlle-Morera L, Doble B, Woodgett J, Cohen P, Smith A (2008) The ground state of embryonic stem cell self-renewal. Nature 453:519
36. Dorey K, Amaya E (2010) FGF signalling: diverse roles during early vertebrate embryogenesis. Development 137:3731–3742
37. Vargel Ö, Zhang Y, Kosim K, Ganter K, Foehr S, Mardenborough Y, Shvartsman M, Enright AJ, Krijgsveld J, Lancrin C (2016) Activation of the TGFβ pathway impairs endothelial to haematopoietic transition. Sci Rep 6:21518
38. Shalaby F, Rossant J, Yamaguchi TP, Gertsenstein M, Wu X-F, Breitman ML, Schuh AC (1995) Failure of blood-island formation and vasculogenesis in Flk-1-deficient mice. Nature 376:62
39. Roberts DM, Kearney JB, Johnson JH, Rosenberg MP, Kumar R, Bautch VL (2004) The vascular endothelial growth factor (VEGF) receptor Flt-1 (VEGFR-1) modulates Flk-1 (VEGFR-2) signaling during blood vessel formation. Am J Pathol 164:1531–1535
40. Hamilton WB, Brickman JM (2014) Erk signaling suppresses embryonic stem cell self-renewal to specify endoderm. Cell Rep 9:2056–2070
41. Liu F, Yang X, Geng M, Huang M (2018) Targeting ERK, an Achilles' Heel of the MAPK pathway, in cancer therapy. Acta Pharm Sin B 8:552–562
42. Lanner F, Rossant J (2010) The role of FGF/Erk signaling in pluripotent cells. Development 137:3351–3360
43. Stanulović VS, Cauchy P, Assi SA, Hoogenkamp M (2017) LMO2 is required for TAL1 DNA binding activity and initiation of definitive haematopoiesis at the haemangioblast stage. Nucleic Acids Res 45:9874–9888
44. Morita R, Suzuki M, Kasahara H, Shimizu N, Shichita T, Sekiya T, Kimura A, Sasaki K-I, Yasukawa H, Yoshimura A (2015) ETS transcription factor ETV2 directly converts human fibroblasts into functional endothelial cells. Proc Natl Acad Sci 112:160–165
45. Liu F, Bhang SH, Arentson E, Sawada A, Kim CK, Kang I, Yu J, Sakurai N, Kim SH, Yoo JJW et al (2013) Enhanced hemangioblast generation and improved vascular repair and regeneration from embryonic stem cells by defined transcription factors. Stem Cell Rep 1:166–182
46. Carithers LJ, Ardlie K, Barcus M, Branton PA, Britton A, Buia SA, Compton CC, DeLuca DS, Peter-Demchok J, Gelfand ET et al (2015) A novel approach to high-quality postmortem tissue procurement: the GTEx project. Biopreserv Biobank 13:311–319